solid-state NMR. Certain values of y are positive (i.e., they increase the magnetic energy) and certain values of y are negative (i.e., they decrease the magnetic energy).

2.40 Summary: Structure and Energetics of Electrons, Vibrations, and Spins

In this chapter we have considered the visualization of the electronic, spin, and vibrational structure of the starting points for photochemical reactions, namely, R* and diradical reactive intermediates, I(D). In particular, a working paradigm has been developed for visualizing the structure of electrons in molecular orbitals, namely, the vibrations of a harmonic oscillator and electron spins as magnetic vectors in a magnetic field. For each structural representation, we can construct state energy diagrams that make it possible to understand the relative ranking of the electronic, vibrational, and magnetic states. Chapter 3 considers the visualization of the photophysical and photochemical transitions of R*, and the way that classical and quantum mechanics provide a deep understanding of all transitions between states from a common conceptual framework.

References

1. (a) P. W. Atkins and R. Friedman, *Molecular Quantum Mechanics*, 5th ed., Oxford University Press, Oxford, UK, 2005. (b) W. Kautzmann, *Quantum Chemistry*, Academic Press, New York, 1957. (c) P. W. Atkins, *Quanta: A Handbook of Concepts*, 2nd ed., Oxford University Press, Oxford, UK, 1991. (d) M. Klessinger and J. Michl, *Excited States and Photochemistry of Organic Molecules*, VCH Publishers, New York, 1995.
2. N. J. Turro, *Angew. Chem. Int. Ed. Engl.* **25**, 882 (1986).
3. L. Salem and C. Rowland, *Angew. Chem. Int. Ed. Engl.* **11**, 92 (1971).
4. W. Kautzmann, *Quantum Chemistry*, Academic Press, New York, 1957, p. 200.
5. P. W. Atkins, *Quanta: A Handbook of Concepts*, 2nd ed., Oxford University Press, Oxford, UK, 1991, p. 153.
6. G. Herzberg, *Spectra of Diatomic Molecules*, Van Nostrand, Princeton, NJ, 1950, p. 91.
7. P. W. Atkins, *Physical Chemistry*, 3rd ed., Oxford University Press, Oxford, UK, 1982, p. 336.
8. K. A. McLauchlan, *Magnetic Resonance*, Oxford University Press, Oxford, UK, 1972, Chapter 1.
9. P. W. Atkins, *Quanta: A Handbook of Concepts*, 2nd ed., Oxford University Press, Oxford, UK, 1991, p. 368.
10. (a) A. Carrington, A. D. McLachlan, *Introduction to Magnetic Resonance*, Harper & Row, New York, 1967. (b) A. L. Buchachenko and V. L. Berdinsky, *Chem. Rev.* **102**, 603 (2002).
11. P. W. Atkins, *Quanta: A Handbook of Concepts*, 2nd ed., Oxford University Press, Oxford, UK, 1991, p. 183.

CHAPTER 3

Transitions between States: Photophysical Processes

3.1 Transitions between States

The state energy diagram (Scheme 1.4) displays the *time-independent* energies for the electronic states of a molecule associated with a given "spatially frozen" nuclear geometry (i.e., the Born–Oppenheimer approximation, which allows us to focus on the *energetics* and *structures* of R and *R). In this chapter, we describe the *time-dependent photophysical transitions* between R and *R in which the energetics and structures change with time. Some of the transitions of interest to organic photophysics, shown in Scheme 3.1, are as follows: (a) radiative absorption of a photon by R to produce *R; (b) emission of a photon from *R to produce R; (c) radiationless transition from *R to produce R and heat; (d) radiationless transitions between electronically excited states, $^{**}R_2$ (higher energy) and *R (lower energy); and (e) radiative transitions between $^*R_2$ (higher energy) and $^*R_1$ (lower energy). *Each of these transitions may involve singlet or triplet states*. Transitions of R and I(D) involving a change of electron spin are discussed in Section 3.12.

Exemplars of structure–reactivity and structure–efficiency relationships for the absorptive and emissive radiative transitions (e.g., $R + h\nu \rightarrow {}^*R$ and ${}^*R \rightarrow R + h\nu$) are covered in Chapter 4. Exemplars of structure–reactivity and structure–efficiency relationships for the radiationless transitions (e.g., ${}^*R \rightarrow R +$ heat and $^{**}R_2 \rightarrow {}^*R_1 +$ heat). Exemplars of the intersystem crossing in I(D) species are covered in Chapter 6. A structural and pictorial model for the primary *photochemical* transitions of Scheme 2.1 (i.e., ${}^*R \rightarrow I$ and ${}^*R \rightarrow F$) are presented in Chapter 6.

According to the laws of quantum mechanics[1] (Section 2.2), the value of any observable property P_1 of a state may be computed from Eq. 3.1 if the wave function of the state Ψ_1 and the mathematical operator P_1 corresponding to the observable property are known. For example, if the electronic energy of a state E_1 is to be computed, the operator P_1 corresponds, in the Born–Oppenheimer approximation, to the classical *repulsive* Coulombic interactions (e^2/r) between two electrons in the field of the fixed

(a) $R + h\nu \rightarrow {}^*R$
(b) ${}^*R \rightarrow R + h\nu$
(c) ${}^*R \rightarrow R + \text{heat}$
(d) ${}^{**}R_2 \rightarrow {}^*R_1 + \text{heat}$
(e) ${}^*R_2 \rightarrow {}^*R_1 + h\nu$

Scheme 3.1 Important photophysical processes in molecular organic photochemistry.

positive nuclear framework. In the matrix element of Eq. 3.1, the two wave functions involved are identical. This means that the matrix element refers to the *property of a single state*, such as the energy of the state.

$$\text{Magnitude of observable property } P_1 = \langle \Psi_1 | P_1 | \Psi_1 \rangle \quad \text{Matrix element} \quad (3.1)$$

In Chapter 2, the most important observable properties P_1 of interest were the state energies (E_n) of the wave functions Ψ_n, where n is the quantum number for the state. In this chapter, we are interested in the rates of transitions between an *initial* state Ψ_1 (the initial state is given the subscript 1) and a second state Ψ_2 (the second state is given the subscript 2). By knowing the wave functions Ψ_1 and Ψ_2 and the laws of quantum mechanics, the rate k of a transition $\Psi_1 \rightarrow \Psi_2$ can be computed from the *square* of a matrix element corresponding to the transition (Eq. 3.2) if $P_{1\rightarrow 2}$, the operator that corresponds to the interaction that triggers the $\Psi_1 \rightarrow \Psi_2$ transition, is known. The rate of a transition that occurs in a single step (called an *elementary step*) is given the symbol k (i.e., the rate constant). The symbol "$\sim$" in an equation means that constants and unessential mathematical features have been omitted for simplicity. Notice that in the matrix element of Eq. 3.1, the two wave functions involved are different, which means that the matrix element refers to a *transition between two states*.

$$k \text{ for the } \Psi_1 \rightarrow \Psi_2 \text{ transition} \quad P_{1\rightarrow 2} \sim \langle \Psi_1 | P_{1\rightarrow 2} | \Psi_2 \rangle^2 \quad (3.2)$$

The rates for each of the transitions in Scheme 3.1 can be estimated by a form of the Eq. 3.2 matrix element. For example, the matrix element given by Eq. 3.3 corresponds to the probability of the transition $R + h\nu \rightarrow {}^*R$ in Scheme 3.1, where the wave functions are represented by the symbols for the initial and final states, $\Psi_1(R)$ and $\Psi_2({}^*R)$, respectively, and $P_{h\nu}$ is the appropriate operator corresponding to the interaction of the R electrons with a photon (or, more precisely, with the electromagnetic field). The use of the square of a matrix element to compute a rate for a transition is at the heart of *Fermi's golden rule* (Eq. 3.8) for transitions between weakly coupled states.

$$k \text{ for the } \Psi_1(R) + h\nu \rightarrow \Psi_2({}^*R) \text{ transition} \sim \langle \Psi_1(R) | P_{h\nu} | \Psi_2({}^*R) \rangle^2 \quad (3.3)$$

In general, the interaction corresponding to the operator $P_{1\rightarrow 2}$ "distorts" the wave function Ψ_1. If this interaction makes Ψ_1 "look like" Ψ_2, a transition between Ψ_1 and Ψ_2 can be "triggered". In the language of wave mechanics, the interaction corresponding to $P_{1\rightarrow 2}$ causes the wave functions Ψ_1 and Ψ_2 to "mix" with one another. Effective

mixing of two waves occurs only under the very special condition of a *resonance* between the two waves Ψ_1 and Ψ_2. *We describe how this notion of resonance due to the mixing of wave functions provides an excellent quantum intuition for the visualization of all of the transitions listed in Scheme 3.1.* For example, the visualization of the resonance corresponding to Eq. 3.3 involves "picturing" how the electromagnetic field of a light wave (a photon, $h\nu$) mixes $\Psi_1(R)$ with $\Psi_2({}^*R)$ and causes a resonance between the two wave functions (when energy and momentum can be conserved). The photon carries the energy and the interaction that is required to achieve the resonance and cause the electronic transition $R + h\nu \rightarrow {}^*R$. Chapter 4 describes and visualizes this resonance in detail with many experimental exemplars.

As with the process for a "zero-order" guess about the nature of the operators (P) that correspond to the properties of states, the mathematical form of the operator $P_{1\rightarrow 2}$, corresponding to the interaction (or perturbation) that causes the transition, is usually made by appealing to a classical model for interactions corresponding to an operator $P_{1\rightarrow 2}$ that can induce transitions $\Psi_1 \rightarrow \Psi_2$. The model for $P_{1\rightarrow 2}$ is then modified to include the appropriate quantum and wave mechanical effects. Once this is done, we can express the operator and wave function in pictorial terms and qualitatively estimate the value of the mathematical integral or matrix element $\langle \Psi_1 | P_{1\rightarrow 2} | \Psi_2 \rangle$ by an equation of the form of Eq. 3.2. This qualitative evaluation of the matrix elements provides useful *selection rules* for the transitions shown in Scheme 3.1. Selection rules serve as a guide to the plausibility of a given transition and the probability of a transition from a state when there are several plausible transitions. In general, $P_{1\rightarrow 2}$ represents the mathematical form of small interactions that can be considered as weak first-order perturbations of the zero-order, or starting, approximation. This result will always be the case when good zero-order electronic wave functions (Ψ_n) have been selected.

3.2 A Starting Point for Modeling Transitions between States

A selection rule is a statement of the plausibility that a state may undergo a specific type of transition under a specific set of circumstances. For the photophysical transitions shown in Scheme 3.1, we seek to develop selection rules that will provide quantum intuition as to whether the probability (or rate) of a transition is closer to the hypothetically "strictly forbidden" (implausible) or "fully allowed" (plausible) limits. The pictorial process for transitions is an extension of the process of visualizing states, except that the notion of time dependence (i.e., transitions between one state and another) is introduced. We begin with a visualization of the wave functions corresponding to the initial state (Ψ_1) and final state (Ψ_2) involved in a transition $\Psi_1 \rightarrow \Psi_2$. With a picture of the wave function of the initial and final states in mind, we apply the rules of quantum mechanics to estimate the (square of the) magnitude of the matrix element (Section 2.5) that describes the qualitative rate of the transition (Eq. 3.2).

To qualitatively estimate the magnitude for the matrix element of Eq. 3.2, we need a picture not only of the wave functions (i.e., the structures) for the initial and final states but also of the operator, $P_{1\rightarrow 2}$. The operator represents the interactions or forces that

most effectively distort the initial state Ψ_1 and make Ψ_1 look like the wave function of the final state Ψ_2. It is natural to accept a physical picture for which transitions occur fastest between two states *when the two states are identical in energy and when the two states involved in the transition "look alike" or can be easily made to look alike as the result of a perturbation* ($P_{1\rightarrow 2}$). This procedure follows the principle of "minimum quantum mechanical reorganization of wave functions" for the fastest transitions. The reorganization includes the energy required to change the molecular structure, motion (phase), and energy required to make Ψ_1 look like the molecular structure, motion (phase), and energy of Ψ_2. By "look alike" we mean "look alike in all respects."

When two classical waves are similar in energy and look very much alike, they are in excellent condition to go into *resonance* and *mix* with one another. Quantum mechanics picks up on this classical idea of the property of waves and states that the wave functions of the two states must have the same energy and look alike in order for *resonance* to occur and for transitions to occur between the two states. If the initial state Ψ_1 goes into a state of resonance with the final state Ψ_2, there is a certain probability that a transition $\Psi_1 \rightarrow \Psi_2$ will occur as the result of the resonance. In a schematic way, the transition $\Psi_1 \rightarrow \Psi_2$ can be viewed as occurring as a "reaction" between the wave function Ψ_1 as a substrate and a perturbation $P_{1\rightarrow 2}$ as a "reagent." The systems interact and go into a "transition state" for which Ψ_2 is mixed into Ψ_1. The transition state contains a "mixture" of Ψ_1 and Ψ_2 and may be described as a "mixed" wave function, $\Psi_1 \pm \Psi_2$. The transition state has a certain probability of collapsing back to Ψ_1 or to Ψ_2. When this happens, a complete transition has occurred.

As was the case for the visualization of state properties, the "true" wave function can be approximated by the product of an electronic wave function Ψ_0, a vibrational wave function χ, and a spin wave function **S**, and transitions between the electronic, vibrational, and spin portions of a transition can be pictured independently.

3.3 Classical Chemical Dynamics: Some Preliminary Comments

We can obtain *classical intuition* about the dynamics of molecular transitions through the concepts of classical mechanical dynamics,[2] which are based on the conservation laws (i.e., the conservation of energy and the conservation of momentum) and Newton's laws of interactions between particles. In particular, Newton's first and third laws for particles are the usual classical starting points when analyzing transitions between electronic states:

1. *The change in the motion of a system is proportional to the forces (interactions) acting on the system.* A central problem in understanding dynamic processes, such as transitions between states, is the identification of the interactions (the operators, $P_{1\rightarrow 2}$, corresponding to the *forces* or *interactions*) involved in changing the motion and the energies of the particles in the initial state Ψ_1 and converting it to the final state Ψ_2. In general, these forces (interactions) are electric or magnetic. Typically, the most important forces involved in causing transitions are electrostatic forces, such as electron–electron (electronic) interactions. Other interactions due to vibrations and spin are usually much weaker. Electronic and vibrational motions can often be visualized as associated oscillating harmonic motions along a conveniently selected axis or a molecular framework. Magnetic motions due to electron spins are associated with circular or rotational motions. A *torque* plays the same role in rotational motion that *force* does in linear motion. More precisely, for linear motion, force is equal to the rate of change of the linear momentum (the back-and-forth motion), whereas for rotational motion, torque is equal to the rate of change of the angular momentum (the twisting circular motion). The concepts of torque and rotational motion are key to understanding and visualizing spin and spin interconversions.
2. *To every action there is always an opposed and equal reaction.* Interactions that cause transitions result from interactions and occur reciprocally. Typically, if we can identify an interaction in one direction of a transition, we can deduce the nature of the interaction in the reverse direction.

The challenge in determining the plausibility of transitions (i.e., $\Psi_1 \rightarrow \Psi_2$) is to identify the *energies* (energy must be conserved) and the *interactions* (forces must be available to change the motions and the structure of the initial system) that are plausible in a particular system, and which of the possible available interactions that conserve energy make the transition $\Psi_1 \rightarrow \Psi_2$ plausible.

3.4 Quantum Dynamics: Transitions between States

In this chapter, we seek to estimate the relative rates of transitions between states by visualizing matrix elements of the form depicted in Eq. 3.2. Recall from Chapter 2 that we described pictorial models for the molecular wave function (Ψ_0) in terms of the approximate electronic (ψ), vibrational (χ), and spin (**S**) wave functions. Our main task in this chapter is to visualize the operators $P_{1\rightarrow 2}$ in Eq. 3.2 and deduce how they operate on the wave functions ψ, χ, and **S** to produce a final value of the matrix element corresponding to the $\Psi_1 \rightarrow \Psi_2$ transition.

3.5 Perturbation Theory[1,3]

Mathematical methods were developed to generate approximate wave functions for complicated organic molecules from simpler systems for which the wave function is known more precisely and which resemble the molecular system of interest as closely as possible. These simpler, approximate wave functions are then "distorted" by a mathematical perturbation (P'), which provides solutions to the wave equation that are closer to the solutions of the true wave function and the true electronic energies. If the exact system resembles the approximate system closely, the distortion required is small and can be considered to be a small "perturbation" of the approximate wave

function. *Perturbation theory* is a mathematical method that provides a recipe for using weak perturbations for mixing wave functions of the approximate system in an appropriate manner so as to achieve better and better approximations of the true system.

Suppose, for example, that we start with an approximate electronic wave function (Ψ_0). The solution of the wave equation (Eq. 2.1) provides the electronic energy (E_0) of Ψ_0. Such approximate wave functions and energies are called zero-order wave functions and zero-order electronic energies, respectively. If a zero-order wave function (Ψ_0) is a reasonable approximation to the true wave function (Ψ), perturbation theory can be employed to "distort" Ψ_0 and its E_0 in the direction of Ψ and the true state energies E_n. Mathematically, the approximate wave function Ψ_0 is said to be *perturbed* (or *corrected*) to look more like the true wave function (Ψ). The key to the successful use of perturbation theory is the judicious selection of zero-order wave functions (Ψ_0), and *the correct physical perturbation to serve as an operator (P') that mixes wave functions.*

A weak perturbation is defined as one that does not significantly change the energies associated with the zero-order wave function. Often, *weak perturbations* are responsible for triggering the transitions shown in Scheme 3.1. A weak perturbation, P', only slightly distorts the zero-order electronic (or vibrational or spin) wave function. This distortion can be interpreted as a "mixing" of the wave functions of the initial state (Ψ_1) and the final state (Ψ_2) as the result of a perturbation whose operator is $P_{1\rightarrow 2}$. As a result of the perturbation-induced mixing, Ψ_1 now contains a certain amount of Ψ_2. That is, there is a resonance between Ψ_1 and Ψ_2. This resonance can be expressed in terms of Eq. 3.4, where λ is a measure of the amount of Ψ_2 that is mixed into Ψ_1 as the result of the perturbation $P_{1\rightarrow 2}$. The value of λ can vary from 0 to 1.

$$\underbrace{\Psi_1 + P_{1\rightarrow 2}}_{\substack{\text{Initial state} \\ \text{+ interaction}}} \rightarrow \underbrace{\Psi_1 \pm \lambda\Psi_2}_{\text{Resonance}} \rightarrow \underbrace{\Psi_2}_{\substack{\text{Transition} \\ \text{to final state}}} \tag{3.4}$$

The basic idea of perturbation theory is that there is a finite probability that after the weak perturbation $P_{1\rightarrow 2}$ has been applied to Ψ_1, the system will be able to achieve resonance so that a certain amount of Ψ_2 will be mixed into Ψ_1. The *mixing coefficient*, λ, is a measure of the extent of distortion of Ψ_1 toward Ψ_2 produced by the perturbation. Before the resonance, the system is approximated as "purely" Ψ_1, and after the resonance and relaxation, the system is approximated as "purely" Ψ_2. In Eq. 3.5, we show how λ is computed.

The modification of the approximate initial wave function Ψ_1 to make it look like the final state Ψ_2 is thus achieved by mixing into it other wave functions of the zero-order system in appropriate proportions through the interactions represented by the operator $P_{1\rightarrow 2}$. If the correct operator (interaction) $P_{1\rightarrow 2}$ has been selected and the proper conditions are present (i.e., the conservation laws are obeyed), the mixing makes Ψ_2 "look like" Ψ_1. The more the mixing makes Ψ_2 look like Ψ_1, the larger the mixing coefficient (λ) becomes, and the faster and more probable is the $\Psi_1 \rightarrow \Psi_2$ transition.

According to perturbation theory, the first-order correction of a wave function Ψ_1 is given by the mixing coefficient λ (Eq. 3.4), which is directly proportional to the strength of the perturbation P', and is inversely proportional to the separation of the energy between the interacting states (ΔE_{12}) being mixed (Eq. 3.5). The first-order wave function is obtained by multiplying Ψ_2 by λ and adding the result to Ψ_1 (Eq. 3.6).

$$\lambda = (\text{strength of the perturbation } P')/(\text{energy of separation of } \Psi_1 \text{ and } \Psi_2) \tag{3.5a}$$

$$\lambda = <\Psi_1|P'|\Psi_2> / \Delta E_{12} \tag{3.5b}$$

$$\Psi_1' \text{ (first-order wave function)} = \Psi_1 + \lambda\Psi_2 \text{ (zero-order wave function).} \tag{3.6}$$

Based on Eqs. 3.5 and 3.6, there are two general rules of perturbation theory that provide us with very important quantum intuition for understanding the role of interactions in promoting effective and fast transitions between electronic states: *(1) the stronger the perturbation P', the stronger the mixing and distortion of the initial wave function Ψ_1, and (2) the smaller the energy separation ΔE between the two interacting wave functions, the stronger the mixing.* For two states (Ψ_1 and Ψ_2) that are widely separated in energy relative to the perturbation, therefore, the system is generally expected to be weakly responsive to any perturbation, and mixing is implausible (in other words, it will be relatively difficult to make Ψ_1 and Ψ_2 look alike, even for a strong perturbation). When a transition involves two states that are very close in energy, on the other hand, the initial system is very sensitive to perturbations and may be strongly perturbed, even by weak perturbations. When Ψ_1 and Ψ_2 have very similar energies, the two systems become "easy to mix" if the correct perturbation is available to operate on the system. The two states (Ψ_1 and Ψ_2) easily transform one into the other even through weak perturbations. This ease of mixing for states that are close in energy is a characteristic *resonance* feature of waves. Classically, it is easier to distort a weak spring (Fig. 2.4, right), but more difficult to distort a strong spring (Fig. 2.4, left) with external perturbations. The same situation holds for a quantum mechanical spring (e.g., vibrating electrons or atoms), because in quantum mechanics a stiff spring has widely separated energy levels (Fig. 2.5, left) and is difficult to perturb (i.e., its wave functions are relatively difficult to mix) compared to a soft spring (Fig. 2.5, right), which has closely spaced energy levels and is easier to perturb (i.e., its wave functions are relatively easy to mix).

The rates of "fully allowed" transitions between electronic states are limited only by the zero-point electronic motion change involved in the transition, provided the nuclear and spin configurations remain constant. Recall from Chapter 1 that we used the time scale for the completion of an orbit by a Bohr electron as a benchmark for the fastest rate of electronic motion. An electron completes its Bohr orbits at a rate of $\sim 10^{15}$–10^{16} s^{-1}, so this sets an approximate upper limit to the zero-point motion of an electronic system. However, if the nuclear and/or spin configurations change during a "fully allowed" electronic transition, the transition will be "rate limited" by the time it takes to change the nuclear or spin configuration, not by the time it takes the electron to make a zero-point motion. In other words, the electronic part of Ψ_1 may have a rate of 10^{15}–10^{16} s^{-1} in "looking like" Ψ_2, but the rate of the $\Psi_1 \rightarrow \Psi_2$ transition may be limited by the time it takes to make the vibrations or spins in the

final state (Ψ_2) "look like" those in the initial state (Ψ_1). Such a view of transition rates provides benchmarks for the maximal rates of various "allowed" transitions. When a rate is slower than the maximal rate, electronic shape and motion, vibrational shape and motion, or spin configuration and motion may serve as kinetic "bottlenecks" in determining transition rates.

To understand molecular kinetics, we must obtain the rate constants (k) for the transitions between the electronic, vibrational, and spin states. It is convenient to consider the observed rate constant for the transition between two states (k_{obs}) in terms of the maximum *possible* rate constant (k^0_{max}) (the zero-point motions determine the rate constant) and the product of the prohibition factors (f) for the electronic, vibrational, and spin aspects of the transitions. In Eq. 3.7, for a given transition from Ψ_1 to Ψ_2, f_e is the prohibition factor associated with the electronic change (the orbital configuration change), f_v is the prohibition factor associated with the nuclear configuration change (usually described as a vibrational change in position or motion), and f_S is the prohibition factor associated with a spin configuration change ($f_S = 1$ for transitions for which there are no spin changes).

Observed Rate Constant		Zero-point Motion-limited Rate Constant		"Fully Allowed Rate"	(3.7)
$\underbrace{k_{obs}}$	$=$	k^0_{max}	$\times$	$\underbrace{f_e \times f_v \times f_S}$	
Prohibition to maximal caused by "selection rules"				Prohibition factors due to changes in electronic, nuclear, or spin configuration	

In most cases k_{obs} is much smaller than k^0_{max}. When *weak* interactions between zero-order states trigger the transition, the rate of $\Psi_1 \rightarrow \Psi_2$ transitions is given by Fermi's golden rule[4] (Eq. 3.8), where ρ is the number of states of Ψ_2 that are of the same energy as Ψ_1 and are capable of being in resonance with Ψ_1 through the perturbation $P'_{1\rightarrow 2}$. The term ρ is referred to as the *density of states that are capable of effectively mixing* Ψ_1 *with* Ψ_2. These are accessible states for which Ψ_1 and Ψ_2 can achieve the same energy during the time scale of the interaction that mixes the states. Pictorially, the higher the density of states for a transition that is capable of responding to a perturbation P', the more statistically probable that a transition will be triggered by any interaction. Fermi's golden rule applies to electronic, vibrational, and spin transitions that are triggered by interactions that are *weak* relative to the energy separations of the states involved. Consequently, the form of Eq. 3.8 shows up a number of times when discussing the rates of transitions that are induced by weak electronic, vibrational, or spin interactions. These weak perturbations include the interaction of the electromagnetic field with the electrons (responsible for the absorption and emission of light) and the interactions between the HOs and LUs of molecules that lead to chemical reaction and energy transfer.

$$k_{obs} \sim \rho[< \Psi_1 | P'_{1\rightarrow 2} | \Psi_2 >]^2 \quad \text{Fermi's golden rule} \tag{3.8}$$

For example, the distortion of the electron cloud of a molecule caused by the (weak) initial interaction of an electromagnetic field can be interpreted quantum mechanically

one or more excited states (*R) to produce a perturbed wave function of R. Since the perturbed wave function of R has wave functions of excited states mixed into it, there is a finite probability of finding the system in an excited state, *R. In the case of an interaction with the electromagnetic field, the matrix element corresponds to the transition dipole moment (Chapter 4). This matrix element may be visualized as being a measure of the extent of the oscillating movement of negative electrical charge along the positive nuclear framework of the molecule as the result of the molecule's interaction with the electric component of the oscillating electromagnetic field. If the extent of the oscillation is great (i.e., if a large transition dipole is generated by the interaction), then the molecule's electrons and the electromagnetic field interact strongly (i.e., the magnitude of the matrix element is large) and the transition rate is high.

Fermi's golden rule provides a basis for the transitions of "selection rules" that are triggered by weak interactions; namely, if the value of the matrix element of Eq. 3.8 is zero (at a defined level of approximation), then the transition is zero and the transition is "forbidden."

In Section 2.3 (Eq. 2.4), we described how to use the Born–Oppenheimer approximation to approximate the true (but mathematically unattainable) wave function Ψ into a product of an electronic (ψ), vibrational (χ), and spin (**S**) wave function. For transitions that do not involve a change in spin (i.e., $\mathbf{S_1} = \mathbf{S_2}$), electronic spin does not provide any prohibition on k_{obs}. In this case, *the rate of transition between* Ψ_1 *and* Ψ_2 *is limited by either the time it takes to make the electronic wave function* ψ_1 *look like* ψ_2 *or the time it takes for the vibrational wave function* χ_1 *to look like* χ_2.

For organic molecules, the most important perturbation for "mixing" electronic wave functions that initially do not look alike is vibrational nuclear motion that is coupled to the orbital motion of the electrons (i.e., vibronic coupling). Let the operator corresponding to vibronic coupling be called P_{vib}; the matrix element for the perturbation that vibrationally mixes ψ_1 and ψ_2 is then given by $< \psi_1 | P_{vib} | \psi_2 >$. It is most important that the electronic wave function of ψ_1 be distorted into a shape that looks like ψ_2 by some vibration that couples the two states. It is this distortion, caused by molecular vibrations, that makes the two wave functions "look alike" and that will allow the transition to occur. When this is true, we need only consider the magnitude of the overlap integral of the vibrational wave functions, $< \chi_1 | \chi_2 >$. The square of the vibrational overlap, $< \chi_1 | \chi_2 >^2$, in Eq. 3.9 is called the *Franck–Condon (FC) factor*. The Franck–Condon factor is a measure of the overlap of the vibrational wave functions of the initial and final states and is mathematically similar to the electron orbital overlap integral (Section 2.14, Eq. 2.20). We show how to obtain a qualitative visualization of the FC factor in Sections 3.10 and 3.11. To summarize, using Fermi's golden rule (Eq. 3.8), k_{obs} is proportional to the square of the product of the vibronic coupling matrix element and the vibrational overlap matrix elements associated with the $\psi_1 \rightarrow \psi_2$ transition, as shown in Eq. 3.9.

$$k_{obs} = \underbrace{\left[\frac{k^0_{max} < \psi_1 | P_{vib} | \psi_2 >^2}{\Delta E^2_{12}}\right]}_{\text{Vibrational coupling}} \times \underbrace{\left[< \chi_1 | \chi_2 >^2\right]}_{\text{Vibrational overlap}} \tag{3.9}$$

When the (radiationless or radiative) transition $\Psi_1 \rightarrow \Psi_2$ involves a change in the spin ($\mathbf{S}_1 \neq \mathbf{S}_2$), which perturbation is most likely to couple states of different spin? In molecular organic photochemistry, the most important transitions involving a change in spin are radiative or radiationless singlet–triplet or triplet–singlet transitions. For organic molecules, the most important perturbation available to make a pair of parallel triplet spins ($\uparrow\uparrow$) look like a pair of antiparallel singlet spins ($\uparrow\downarrow$) is the coupling of the electron spin motion with the electron orbital motion (termed *spin–orbit coupling*), which takes one of the parallel electron spins of a singlet state ($\uparrow\uparrow$) and twists it or flips it, making the spins antiparallel ($\uparrow\downarrow$). The terms "parallel" and "antiparallel" are approximations used here for simplicity; recall from Section 2.28 that the 3D representation of spin vectors is a more accurate description and is required when we analyze spin transitions in Section 3.12.

Let us label the operator that induced spin–orbit coupling as P_{so}, and the matrix element for the transition as $< \psi_1 | P_{so} | \psi_2 >$. This matrix element is a measure of the strength (or the energy) of the spin–orbit interactions. For simplicity, the spin wave functions, $\mathbf{S}_1$ and $\mathbf{S}_2$, need not be considered explicitly: recall from Table 2.1 that we use the symbols α and β to represent the wave functions of a spin up ($\uparrow$) and spin down ($\downarrow$), respectively. For transitions that involve a change in spin, we can modify Eq. 3.9 to produce Eq. 3.10, which includes the spin change prohibition.

$$k_{obs} = \underbrace{\left[\frac{k^0_{max} < \psi_1 | P_{vib} | \psi_2 >^2}{\Delta E^2_{12}}\right]}_{\text{Vibrational coupling}} \times \underbrace{\left[\frac{< \psi_1 | P_{so} | \psi_2 >^2}{\Delta E^2_{12}}\right]}_{\text{Spin–orbital coupling}} \times \underbrace{\left[< \chi_1 | \chi_2 >^2\right]}_{\substack{\text{Vibrational overlap} \\ \text{Franck-Condon factors}}} \tag{3.10}$$

3.6 The Spirit of Selection Rules for Transition Probabilities

As a starting approximation, a $\Psi_1 \rightarrow \Psi_2$ transition is "forbidden" (implausible) if the value of the matrix element equals zero, and the transition is "allowed" if the value of the matrix element is finite. The matrix element for a transition probability for the $\Psi_1 \rightarrow \Psi_2$ transition, $< \Psi_1 | P_{1\rightarrow 2} | \Psi_2 >$, may be calculated for a certain set of zero-order assumptions that assign an initial idealized symmetry for the wave functions for the electrons, nuclei, and spins (ψ, χ, and $\mathbf{S}$) and a selected operator ($P_{1\rightarrow 2}$) that is assumed to trigger the transition. If the computed matrix element for the transition probability equals zero, the transition is strictly forbidden in the zero-order approximation. The plausibility of the transition in first order will depend on whether an interaction (e.g., vibronic or spin–orbit) exists that can overcome the forbidden character of the zero-order approximation.

When the approximate wave functions Ψ_1 and Ψ_2 possess a more realistic non-ideal symmetry, or when previously ignored forces and a different operator have been included, a *new* calculation of the matrix element may yield a first-order correction, and the value of the matrix element generally will be nonzero. If the transition probability corresponding to the matrix element is still small (e.g., < 1% of the maximum transition probability), then the process is "weakly allowed" (or *implausible*) in the sense that the rate of the process is not expected to compete with other fast transitions from the initial state. If the matrix element computed by the new calculation for the transition is large (e.g., close to the maximum transition rate, f, in Eq. 3.7), then the transition can be classified as "strongly allowed" (or *probable*) in the sense that its rate is expected to be among the fastest of the plausible transitions. Such qualitative descriptions can provide only a rough feeling for transition probabilities. Indeed, sometimes the breakdown of selection rules is so severe that the magnitude of the "forbidden" transition probability approaches that of the "allowed" transition probability. When this occurs, we have selected a poor zero-order starting point (the wave function Ψ_0 or the operator P) for our evaluation of the transition probability.

3.7 Nuclear Vibrational Motion As a Trigger for Electronic Transitions. Vibronic Coupling and Vibronic States: The Effect of Nuclear Motion on Electronic Energy and Electronic Structure[5]

For *spin-allowed electronic* transitions between Ψ_1 and Ψ_2, we need to devise a paradigm for evaluating the matrix elements for vibrational coupling of the electronic states of Ψ_1 and Ψ_2 (i.e., vibronic coupling). The goal is to estimate how the vibrational wave functions (Section 2.19) for spin-allowed transitions influence the rate of both radiative and radiationless electronic transitions (Scheme 3.1). The FC factors, $< \chi_1 | \chi_2 >^2$, are a measure of the similarity of the vibrational wave functions of Ψ_1 and Ψ_2 and are critical in determining whether a transition is allowed or forbidden in first order.

The Born–Oppenheimer approximation (Section 2.3, Eq. 2.4) allows the generation of a zero-order description of the electronic structure and electronic energy of a molecule, based on an assumed frozen, *nonvibrating* nuclear geometry. We must consider the effect of nuclear vibrational motion on the electronic structure and electronic energy of a molecule and how this vibrational motion can serve as a perturbation that mixes electronic wave functions and how this mixing can induce transitions between electronic states. Our goal is to replace the pure, classical "vibrationless" molecule with a vibrating molecule and to be able to visualize how this motion will modify our zero-order model. We call the states of a vibrating molecule "vibronic" states rather than pure "electronic" states, because *vibrations are constantly serving as a source of mixing of electronic states, especially electronic states that are of similar or identical energy in zero order.* The basic concept is that the vibrations of a molecule will distort the zero-order electronic wave function only slightly, therefore serving as a weak perturbation on the approximate wave function, but that certain vibrations will distort the approximate function so that it looks like the wave function of other electronic states to which transitions may occur. Again assuming only weak interactions, the *energy* E_V of a vibronic perturbation (from perturbation theory) is given by Eq. 3.11a. From Fermi's golden rule for weak interactions (Eq. 3.8), the *rate* of the transition

from $\Psi_1 \rightarrow \Psi_2$ is proportional to the square of the matrix element (where $P'_{1\rightarrow 2}$ is replaced by P_{vib}) for the transition multiplied by the density of states (ρ) capable of being mixed by P_{vib} during the time scale of the perturbation (Eq. 3.11b).

$$E_V = <\Psi_1|P_{vib}|\Psi_2>^2 / \Delta E_{12} \tag{3.11a}$$

$$k_{obs} \sim \rho <\Psi_1|P_{vib}|\Psi_2>^2 \tag{3.11b}$$

In Eq. 3.11a, Ψ_1 and Ψ_2 are two pure zero-order electronic states that are "mixed" by P_{vib} and ΔE_{12} is the energy difference between the zero-order electronic states that are being mixed by the vibronic interaction.

We have described interactions that allow the use of Fermi's golden rule as "weak" perturbations. At this point, we provide some numerical benchmarks for the values of the energy separations (ΔE_{12}) that are involved in the vibronic mixing of electronic states. What do we mean by a small or large value of ΔE_{12}? We know from perturbation theory (Eqs. 3.5 and 3.6) that if ΔE_{12} is large, the mixing (the value of λ) of the states will be small, and if ΔE_{12} is small, the mixing of the two states will be large. Intuitively, what we mean by small or large has to do with how the vibronic mixing energy (E_V) compares to the energy separation (ΔE_{12}) of the electronic states that are being mixed by vibronic interactions. If E_V is small (i.e., a few percent) compared to ΔE_{12}, the mixing of the states is expected to be small. In general, for organic molecules, the value of E_V is on the order of vibrational energies (Section 2.19), which range from $\sim$ 10 kcal mol^{-1} for X—H stretching vibrations to $\sim$ 1 kcal mol^{-1} for C—C—C bending vibrations. As a result, X—H vibrations can be very effective in mixing electronic states.

Vibronic interactions do not significantly mix electronic states whose energy separation (ΔE_{12}) is 50 kcal mol^{-1} or greater. The energy gaps between the ground state (R) and lowest excited states (*R) of most organic molecules are > 50 kcal mol^{-1}, so the vibronic mixing of R and *R is weak. This weak vibronic coupling is the reason that the Born–Oppenheimer approximation works so well for ground-state molecules; that is, vibrations in the ground state do not mix electronically excited states very effectively because the electronic energy gap between R and *R is much larger than the vibrational energies.

However, vibronic interactions are much more likely to be significant in mixing zero-order electronically *excited* states ($^*R_2$ and $^*R_1$), since ΔE_{12} between excited states is often on the order of only several kilocalories per mole or less, so excited states are typically packed together with much smaller energy gaps than the energy gaps that separate *R from R. *When electronic states are separated by small energy gaps, the electronic energy and electronic structure of the states may vary considerably during a vibration.* Thus, vibrational motion of the appropriate type (e.g., a motion that couples two electronic states that are close in energy) can be very effective in mixing excited states. Such effects are of great importance in triggering and, therefore, determining the rates of transitions from excited states.

The importance of similar energy states in determining the rates of transitions is apparent in Fermi's golden rule, where k_{obs} depends on the density of states (ρ) that have the same energy in both Ψ_1 and Ψ_2 (Eqs. 3.8 and 3.11b). We also conclude that

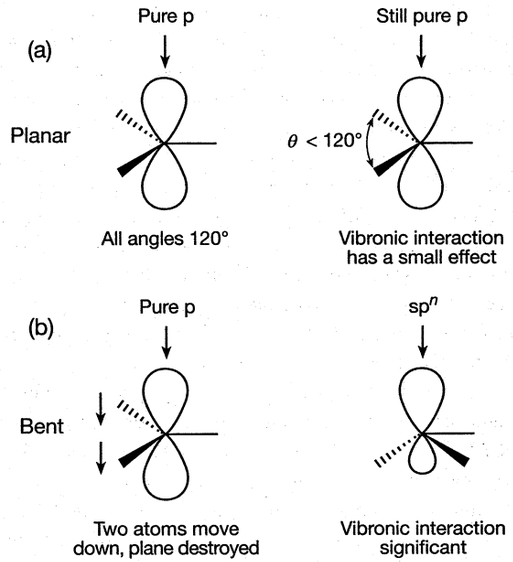

Figure 3.1 The effect of vibronic motion on the hybridization of a p orbital.

electronic transitions from any *R, both radiative and radiationless, depend on the ability of certain kinds of vibrations to couple the electronic wave function of *R with the wave functions of other states, particularly with other excited states.

As a simple exemplar (Fig. 3.1) of the effect of vibrational motion on the electronic orbital energy, consider the vibrations of a carbon atom that is bound to three other atoms (e.g., a methyl group as a radical, anion, or carbonium ion). When the system is planar and the angles between the atoms are 120°, the carbon atom is a pure sp^2 hybrid and possesses a p orbital that serves as a "free valence" orbital. What happens to the shape and energy of this free valence orbital as the molecule vibrates? If the vibrations do not destroy the planar geometry (i.e., the H—C—H angle changes, but the system remains planar), the hybridization remains sp^2 and the spatial distribution of the free valence orbital above and below the plane must be *identical* because of the symmetry plane that contains all four atoms (Fig. 3.1a). In other words, if we put electrons into the free valence orbital, the electron density would have to be the same above and below the symmetry plane, since all conceivable interactions on one side of the plane are identical to those on the other side. In effect, *the* p *orbital remains essentially "pure* p*" during the in-plane bending vibration. Furthermore, since the system remains planar during the vibration, the energy of the orbital is not expected to change significantly as it executes the in-plane vibration.* We say that there is weak vibronic coupling of electronic (p-orbital) and vibrational (in-plane) motions so that distortion of the p orbital induced by vibrations is small.

Now, consider a bending (umbrella-flipping) vibration that *breaks* the planar symmetry of the molecule and causes a change in the hybridization of the carbon atom (Fig. 3.1b). Intuitively, we expect the "pure p" orbital to change its shape in response to the fact that more electron density (due to the electrons in the bonds) is on one side of the plane. We say that a *rehybridization* of the carbon atom occurs, and that the "pure p" orbital begins to take on some s character; that is, *the out-of-plane vibration converts the pure* p *orbital into an* sp^n *orbital*, where n is a measure of the "p character" remaining. Since an s orbital is considerably lower in energy than a pure p orbital, an sp^n orbital will be lower in energy than a p orbital because the sp^n orbital has acquired some s character. Thus, the mixing due to out-of-plane vibrational motion can change the energy of the free valence orbital significantly.

In the extreme situation for sp^n, where $n = 3$, the out-of-plane vibration causes a continual oscillating electronic change, p (planar) $\leftrightarrow$ sp^3 (pyramidal), as pyramidal shapes interconvert through the planar shape. A significant vibronic coupling of the electronic and nuclear motion occurs due to this vibration, causing the value of n to oscillate between 2 and 3. Now, if the initial state (Ψ_1) is a pure p wave function and the final state (Ψ_2) is a pure sp^3 state, the out-of-plane vibrational motion makes Ψ_1 "look like" Ψ_2, but the in-plane vibrational motion does not, because the in-plane bending vibration does not introduce any s character into the p orbital. In other words, the out-of-plane vibrational motion "mixes" the hybridization of the free valence orbital, but the in-plane vibrational motion does not. In a convenient shorthand, we can write Ψ_1(p, planar) $\leftrightarrow$ $\Psi_2(sp^3$, pyramidal). If the operator that describes the in-plane (ip) vibronic interaction is called P_{ip} and the operator that describes the out-of-plane (op) vibronic interaction is called P_{op}, then the matrix element for in-plane vibronic mixing, $< \Psi_1 | P_{ip} | \Psi_2 >$, equals 0, and the matrix element for out-of-plane vibronic mixing, $< \Psi_1 | P_{op} | \Psi_2 >$, is finite in this case.

To summarize, some, but not all, vibrations are capable of perturbing the electronic wave functions and the electronic energy of zero-order electronic states. The energy difference of the zero-order electronic levels and vibronic levels may be small relative to the total electronic energy, yet the matrix element $< \Psi_1 | P_{vib} | \Psi_2 >$ may "provide a first-order mechanism" for the transition from one vibronic state to another, even though the electronic transition is strictly forbidden (i.e., $< \Psi_1 | P | \Psi_2 > = 0$) in the zero-order approximation.

3.8 The Effect of Vibrations on Transitions between Electronic States: The Franck–Condon Principle

The rates of transitions between electronic states ($\Psi_1 \rightarrow \Psi_2$) can be limited by either the rate at which the electrons in Ψ_1 can adjust to the nuclear geometry of Ψ_2, or the rate at which the nuclear geometry of Ψ_1 can adjust to the nuclear geometry of Ψ_2.

The Born–Oppenheimer approximation (Section 2.3) assumes that electron motion is so much faster than nuclear motion that the electrons "instantly" adjust to any change in the position of the nuclei in space. Since an electron jump between orbitals

(Section 1.13) generally takes $\sim 10^{-15}$–10^{-16} s to occur, whereas nuclear vibrations take $\sim 10^{-13}$–10^{-14} s to occur, the electron jump is generally much faster and will not be rate determining for transitions between two electronic states, $\Psi_1 \rightarrow \Psi_2$. Thus, the transition rate between electronic states (of the same spin) is limited by the ability of the system to adjust to the nuclear configuration and motion *after* the change in the electronic distribution of Ψ_1 to that of Ψ_2. *The rate of transitions induced by vibrations (nuclear motion) depends not only on how much the electronic distributions of the initial and final states look alike but also on how much the nuclear configuration and motion in the initial and final states look alike.*

Expressed in classical terms, the FC principle states that *because nuclei are much more massive than electrons (the mass of a proton is* ~ 1000 *times the mass of an electron), an electronic transition from one orbital to another takes place while the massive, higher-inertia nuclei are essentially stationary.* This means that, at the instant that a radiationless or radiative transition takes place between Ψ_1 and Ψ_2 (e.g., for any of the transitions shown in Scheme 3.1), the nuclear geometry of the massive nuclei momentarily remains fixed while the new electron configuration readjusts from that Ψ_1 to that of Ψ_2. After completion of the electronic transition, the nuclei experience the new electronic negative force field of Ψ_2 and begin to move and swing back and forth from the geometry of Ψ_1 until they adjust their nuclear geometry to that of Ψ_2. From the FC principle, we conclude that the conversion of electronic energy into vibrational energy is likely to be the rate-determining step in an electronic transition between states of significantly different nuclear geometry (but of the same spin).

Expressed in quantum mechanical terms, the FC principle states that *the most probable transitions between electronic states occur when the wave function of the initial vibrational state* (χ_1) *most closely resembles the wave function of the final vibrational state* (χ_2). In analogy to the orbital overlap integral $< \psi_1 | \psi_2 >$ (Section 2.14), which defines the extent of the mathematical orbital overlap for a pair of electronic wave functions or a set of orbitals, we define the vibrational overlap integral in terms of the extent of overlap for a pair of vibrational wave functions (χ_1 and χ_2) and use the symbol $< \chi_1 | \chi_2 >$ to indicate the degree of the overlap integral of the two vibrational wave functions, χ_1 and χ_2. Since two wave functions generally have a greater resemblance (i.e., look more alike) when the vibrational overlap integral $< \chi_1 | \chi_2 >$ is closer to 1 (the maximum value for complete overlap), the larger the value of the integral, the more probable the vibronic transition. From Eq. 3.9, the rate constant (k_{obs}) for the $\Psi_1 \rightarrow \Psi_2$ transition is proportional to $< \chi_1 | \chi_2 >^2$. We can now understand why $< \chi_1 | \chi_2 >^2$ in Eq. 3.9 is called the "Franck–Condon" factor.

In the following sections, we demonstrate that the FC principle provides a useful visualization of both radiative and radiationless electronic transitions. For radiative transitions, the *motions and geometries* of nuclei do not change during the time it takes for a photon to "interact with" and to be "absorbed," thus causing an electron to jump from one orbital to another. For radiationless transitions, nuclear *motions and geometries* do not change during the time it takes an electron to jump from one orbital to another.

3.9 A Classical and Semiclassical Harmonic Oscillator Model of the Franck–Condon Principle for Radiative Transitions ($R + h\nu \rightarrow {}^*R$ and ${}^*R \rightarrow R + h\nu$)

In the classical harmonic oscillator approximation (Section 2.16), the energies of the vibrations of diatomic molecules were discussed in terms of a parabola in which the potential energy (PE) of the system was displayed as a function of the displacement (Δr) from the equilibrium separation of the atoms (Eq. 2.24 and Figs. 2.3 and 2.4). The harmonic oscillator approximation for molecular vibrations applies to both ground states (R) and excited states (*R) and can be used as a starting point for both radiationless and radiative photophysical transitions. First, let us consider how the FC principle and FC factors apply to a radiative transition between two states in terms of the harmonic oscillator model.[6]

Figure 3.2 shows classical PE curves for a diatomic molecule (X—Y) that behaves as a harmonic oscillator. The top half of Fig. 3.2 is a representation of a classical harmonic oscillator for which one of the vibrating masses (X) is very large (X is attached to the left of the spring), and the other vibrating mass (Y) is much lighter (Y is attached to the right of the spring). This diatomic molecule can be viewed as a vibrating ball attached to a spring, which is affixed to a wall. This would be analogous to a light atom (the ball) bonded to a much heavier atom (the wall), for example, a C—H vibration where the carbon atom is analogous to the massive wall and the hydrogen atom is analogous to the light ball. Most of the motion of the two atoms is due to the movement in space of the lighter particle (the H atom).

Three PE curves are shown in Fig. 3.2 for three different situations with respect to an initial nuclear geometry of an R state relative to that of an *R state. In Fig. 3.2a, the equilibrium nuclear separation (r_{XY}) of R is essentially identical to the equilibrium nuclear separation (${}^*r_{XY}$) of the electronically excited *R molecule. In Fig. 3.2b, r_{XY} of R is slightly different from ${}^*r_{XY}$ of the *R molecule, with ${}^*r_{XY}$ being slightly longer because of (an assumed) slightly weaker bond resulting from electronic excitation and the placement of an electron in an antibonding orbital. In Fig. 3.2c, r_{XY} of R is considerably different from ${}^*r_{XY}$ of the *R molecule, with ${}^*r_{XY}$ being considerably longer because of the much weaker bond resulting from electronic excitation to put an electron into an antibonding orbital. The difference in excess vibrational energy (ΔE_{vib}) increases as the difference ($\Delta r = |{}^*r_{XY} - r_{XY}|$) in the equilibrium separations of R and *R increases. It is zero for the case in Fig. 3.2a, small for the case in Fig. 3.2b, and large for the case in Fig. 3.2c.

For each case in Fig. 3.2, a line is drawn vertically from the initial R state and intersects the upper PE curve at the point that will be the turning point in the *R state. This line represents a *vertical* electronic transition from R to *R. Radiative transitions are called vertical transitions with respect to nuclear geometry, since the nuclear geometry (r_{XY}, the horizontal axis) is fixed during the electronic transition. The length of the line representing the vertical electronic transition corresponds to the difference in energy between R and *R that is absorbed in the transition, that is, the energy of the absorbed photon is $|E_R - E_{*R}| = \Delta E = h\nu$.

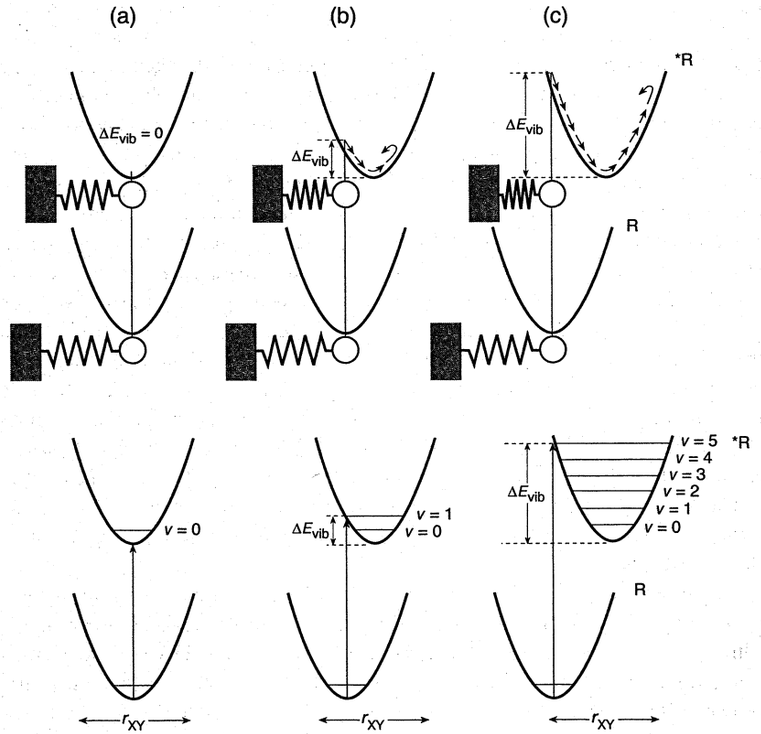

Figure 3.2 A mechanical representation of the Franck–Condon principle for radiative transitions of a diatomic molecule, XY. The motion of a point representing the vibrational motion of two atoms is shown by a sequence of arrows along the PE curve for the vibration in the top set of curves.

Now, let us consider how the FC principle influences a radiative $HO + h\nu \rightarrow LU$ orbital transition that takes R to *R. The time scale for photon absorption is on the order of 10^{-15}–10^{-16} s. According to the FC principle, the nuclear geometry (i.e., the separation of the two atoms) does not change during the time scale of an electronic transition or orbital jump; that is, immediately after the electronic transition, $r_{XY} = {}^*r_{XY}$. Thus, the geometry produced at the instance of the electronic transition on the upper surface by a radiative transition from a ground R state to an *R state is governed by the relative positions of the PE surfaces controlling the vibrational motion of R and *R.

If, for simplicity, we assume that the PE curves have similar shapes, and that the minimum of one curve lies directly over the minimum of the other (Fig. 3.2a), the Franck–Condon principle states that the most probable radiative electronic transitions would be from an initial state that has a separation of r_{XY} in R that is identical to

the separation (r_{XY}) of the excited state *R. Since the two curves are assumed to lie exactly over one another, the most favored Franck–Condon transition will occur from the minimum of the ground surface to the minimum of the excited surface, that is, $R(v = 0) + h\nu \rightarrow {}^*R(v = 0)$. This situation is typical of the absorption of light to induce a $\pi \rightarrow \pi^*$ transition of aromatic hydrocarbons that have many bonding π electrons, so that the excitation of one π electron to a π^* orbital does not significantly change the structure of *R compared to R (Chapter 4). To a good approximation, therefore, we may regard the *absorption* of a photon as occurring from the *most probable* nuclear configuration of the ground state (R), which is the static, equilibrium arrangement of the nuclei in the classical model and is characterized by a separation r_{XY}. Based on Fig. 3.2, there is no excess vibrational energy produced by the transition.

By using the exemplar of Fig. 3.2b, let us consider the absorption of light from the HO of formaldehyde (the n_O orbital) to its LU (the π^* orbital). At the instance of completion of the electronic transition is complete, the nuclei are still in the same ground–state equilibrium (planar) geometry that they were before the transition, because the electronic jump occurs much faster than the nuclear vibrations. However, as the result of the orbital transition and the occupation of a π^* orbital, the electron density of *R about the nuclei is different from the electron density of R about the nuclei. Therefore, *R relaxes to a new geometry (that turns out to be a pyramidally shaped $H_2C{=}O$).

Figure 3.2c is an exemplar of a system that undergoes a very large structural change upon going from R to *R. The $\pi \rightarrow \pi^*$ excitation of ethylene is one such example. Although the equilibrium geometry of the ground state for ethylene (R) is planar, the equilibrium geometry of the excited state for ethylene (*R) is strongly twisted, leading to a large change in the equilibrium geometry of *R compared to R.

Now, let us consider the effect of the Franck–Condon principle on the excess of vibrational energy that is produced in *R upon absorption of a photon. In Fig. 3.2a, where the initial and final geometries of R and *R are assumed to be identical, there is no significant change in vibrational properties resulting from electronic excitation ($R + h\nu \rightarrow {}^*R$), so *R is produced with no excess vibrational energy. However, in Fig. 3.2b and c, the electronic transition initially produces an *R state that is both a *vibrationally excited and an electronically excited species* as the result of the new force field experienced by the originally stationary nuclei of R. A few femtoseconds after the $R \rightarrow {}^*R$ transition, the atoms in *R will suddenly burst into a new vibrational motion in response to the new electronic force field of *R.

In the case of the n,π^* state of $H_2C{=}O$, an electron has been promoted into a π^* orbital, which will tend to make the C—O bond begin to vibrate and to stretch and become longer. This new force, provided by the sudden perturbation of the removal of an n electron and of the creation of a π^* electron, will induce a vibration along the C—O bond. The new vibrational motion of the molecule in $^*R(n,\pi^*)$ may be described in terms of a *representative point*, which represents the value of the internuclear separation and is constrained to follow the PE curve and execute harmonic oscillation.

The excess vibrational motion produced by absorption of a photon is indicated by the set of arrows on the PE surface in Fig. 3.2b and c. The maximum velocity

of the motion of the representative point on the PE surface depends on the excess vibrational kinetic energy produced upon electronic excitation. The greater the excess vibrational motion produced by Franck–Condon excitation, the greater the velocity of vibrational motion produced immediately after electronic excitation. In the case of the $\pi \rightarrow \pi^*$ transition of ethylene, the loss of a π electron and the creation of a π^* electron strongly reduces the C=C bonding and essentially breaks the π double bond and creates a C—C single bond in *R. The new electronic distribution in the π,π^* state favors a twisting about the essentially C—C single bond and an equilibrium geometry that favors the two CH_2 groups perpendicular to each other rather than in the same plane (this situation is discussed in detail in Chapter 6).

For the classical case of Fig. 3.2b and c, *it follows that the original nuclear geometry of the ground state is a turning point of the new vibrational motion in the excited state, and that vibrational energy is stored by the molecule in the excited state.* Since the total energy of a harmonic oscillation is constant in the absence of friction, any PE lost as the spring decompresses is turned into the kinetic energy (KE) of the two masses attached to the spring, which sets the representative point into harmonic oscillation. Therefore, the PE at the turning points, E_{vib}, determines the energy at all displacements for that mode of oscillation. The greater the amount of vibrational energy that is produced in *R upon photoexcitation, the greater the amplitude of the vibration of *R.

Now, let us examine a "semiclassical" model (Fig. 3.2, bottom) that considers the effect of quantization of the vibrational levels of the harmonic oscillator and of zero-point motion on the classical model for a radiative electronic transition (we will consider the wave character of vibrations in Section 3.10). In Section 2.18, we learned that one of the effects of quantization on the harmonic oscillator is that only certain vibrational energies are allowed. In a semiclassical model, therefore, the classical PE curves must be replaced by PE curves displaying the quantized vibrational levels, each with a vibrational quantum number, $v = 0$. For example, Fig. 3.2a (bottom) shows the ground-state PE curve with a horizontal level corresponding to the $v = 0$ vibrational level. This level corresponds to a small range of nuclear geometries, determined by the zero-point vibrational motion, with the classical equilibrium geometry at the center of the vibration. *Radiative transitions from $v = 0$ will therefore not be initiated from a single geometry but will be initiated from a range of geometries that are explored during the zero-point motion of the vibration.* In Fig. 3.2a (bottom), the most probable transition is from the $v = 0$ level of R to the $v = 0$ level of *R. In Fig. 3.2b, the most probable transition is from the $v = 0$ level of R to the $v = 1$ level of *R. In Fig. 3.2c, the most probable transition is from the $v = 0$ of R to the $v = 5$ level of *R. As we go from Fig. 3.2a to b to c, the amount of excess vibrational excitation produced in *R by the electronic transition increases.

The final step in our visualization of the FC principle and radiative transitions is to determine how to picture the wave functions corresponding to the vibrational levels of R and *R. From this picture, we will see that the mathematical form of the vibrational wave functions of R and *R controls the probability of both radiative and radiationless electronic transitions between vibrational levels.

3.10 A Quantum Mechanical Interpretation of the Franck–Condon Principle and Radiative Transitions[7]

Recall from Section 2.19 that according to quantum mechanics, the classical concept of the precise position of nuclei in space and associated vibrational motion is replaced by the concept of a *vibrational wave function*, χ, which describes the nuclear configuration and nuclear vibrational momentum during a vibration. In the language of classical mechanics, the FC principle states that the most probable electronic transitions will occur between those states possessing a similar nuclear configuration and vibrational momentum at the instant of an electronic transition. In the language of quantum mechanics, the FC principle states that the most probable electronic transitions are those that possess vibrational wave functions that look most alike in the initial (χ_1) and final (χ_2) states at the instant of the electronic transition.

A measure of how much two states undergoing a transition "look alike" is given by the overlap integral (called the FC integral) of the vibrational wave functions of the two states, $< \chi_1|\chi_2 >$. A net mathematical positive overlap of vibrational wave functions means that the initial and final vibrational states possess similar nuclear configurations and momentum in some region of space. Eq. 3.11b shows that the matrix element for any electronic transition is directly related to *the square* of the vibrational overlap integral (i.e., the FC factor, $< \chi_1|\chi_2 >^2$, Eq. 3.9).

The larger the FC factor, the greater the net constructive overlap of the vibrational wave functions, the more similar χ_1 is to χ_2, and the more probable the transition. Thus, an understanding of the factors controlling the magnitude of $< \chi_1|\chi_2 >^2$ is crucial for an understanding of the probabilities of radiative and radiationless transitions between electronic states. The FC factor may be considered a sort of nuclear "reorganization energy," similar to entropy, that is required for an electronic transition to occur. Recall that high organization implies a small degree of entropy and low organization implies a large degree of entropy. The greater the reorganization energy, the smaller the FC factor and the slower the electronic transition. The larger the FC factor, the smaller the reorganization energy and the more probable the electronic transition.

The FC principle provides a selection rule for the *relative probability of vibronic transitions*. Quantitatively, for *radiative* transitions of absorption or emission the FC factor ($< \chi_1|\chi_2 >^2$) *governs* the relative intensities of vibrational bands in electronic absorption and emission spectra. The Franck–Condon factor is also important in determining the rates of *radiationless* transitions between electronic states. Since the value of $< \chi_1|\chi_2 >^2$ parallels that of $< \chi_1|\chi_2 >$, we need only consider the FC integral itself, rather than its square, for qualitative discussions of transition probabilities. We can obtain considerable quantum intuition simply by noting that the larger the difference in the vibrational quantum numbers for χ_1 compared to χ_2, the more likely it is that the equilibrium shape and/or momentum of the initial and the final states are different, and the more difficult and slower and less probable the transition $\chi_1 \rightarrow \chi_2$ will be. Indeed, this is exactly the result anticipated from the classical FC principle. In other words, the magnitude of the integral $< \chi_1|\chi_2 >$ is related to the probability that an initial state χ_1 will have the same shape and momentum as χ_2. If this probability is high, the transition rate will be high also.

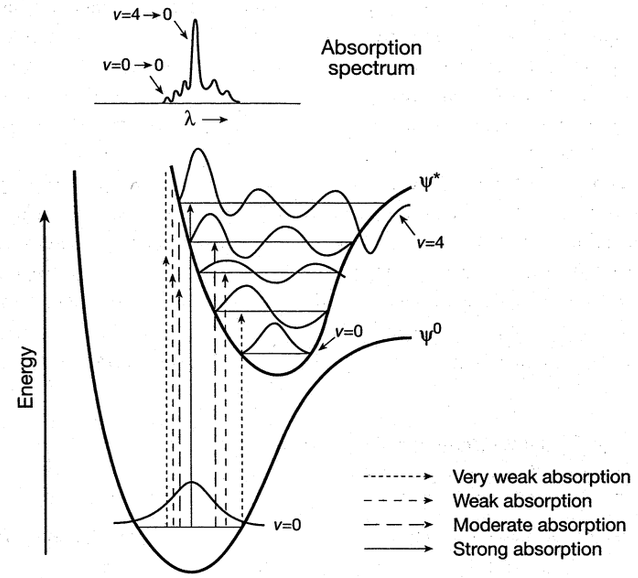

Figure 3.3 Representation of the quantum mechanical Franck–Condon interpretation of the absorption of light.

Consider Fig. 3.3, a schematic representation of the quantum mechanical basis of the FC principle for a radiative transition from an initial ground electronic state ψ_1 (i.e., R) to a final electronic excited state $^*\psi_2$ (i.e., *R). Absorption of a photon is assumed to start from the lowest-energy, $v = 0$ level of ψ_1, since this state is usually the most populated vibrational level in the ground state of R. According to the FC principle, the most likely radiative transition from $v = 0$ of ψ_1 to a vibrational level of $^*\psi_2$ will correspond to a vertical transition for which the overlap integral $< \chi_1|\chi_2 >$ is maximal. By inspection of Fig. 3.3, the overlap integral ($< \chi_1|\chi_2 >$) is maximal for the $v = 0 \rightarrow v = 4$ transition (χ_1 is positive everywhere and χ_2 is strongly positive vertically above the maximum of χ_1). Transitions from $v = 0$ to other vibrational levels of $^*\psi_2$ (e.g., from $v = 0$ of ψ_1 to $v = 3$ and $v = 5$ of $^*\psi_2$) may occur, but with lower probability because of the smaller overlap of χ_1 and χ_2 for these vertical transitions. A possible resulting absorption spectrum showing schematically how the intensities for an experimental absorption spectrum would vary is shown in Fig. 3.3, above the PE curves for ψ_1 and $^*\psi_2$. The intensities of the transitions are proportional to the values of the FC overlap integrals, with the $v = 0 \rightarrow v = 4$ transition being maximal.

The same general ideas of the FC principle apply to emission, except now *the important overlap is between the χ corresponding to $v = 0$ of $^*\psi_2$ (the equilibrium position of the excited state) and the various vibrational levels, χ_i,* of ψ_1. Chapter 4 discusses experimental examples of the FC principle for radiative transitions.

In Section 3.13, we shall seek quantum intuition concerning transitions involving electron spins in electronic radiative and radiationless processes. In this case, in addition to the Franck–Condon factors for vibrations, we are concerned with the overlap of two types of spin wave functions (**S**), the wave functions for singlets and triplets corresponding to *R. We have seen from the vector model discussed in Section 2.27 that the wave functions for singlets (with antiparallel spins $\uparrow\downarrow$) and triplets (with parallel spins $\uparrow\uparrow$) do not look alike at all! When two spin wave functions do not look alike, a *magnetic* perturbation, such as spin–orbit coupling, is required to distort the initial spin state to make it look like the final spin state and thereby induce a radiationless transition or a spin-forbidden radiative transition. The discussion of FC factors on radiative and radiationless transitions described in Section 3.11 are the same for transitions involving a spin change, but in addition to a good FC factor, transitions involving a spin change require simultaneously significant spin–orbit coupling.

3.11 The Franck–Condon Principle and Radiationless Transitions (*R → R + heat)[8]

The original FC principle stated that there is a preference for "vertical" jumps between PE curves for the representative point of a molecular system during a *radiative* transition. The classical and quantum mechanical ideas behind the FC principle for *radiative transitions* can be extended to *radiationless* transitions. The basic idea is the same for radiative and radiationless transitions; namely, (1) a small change in the initial and final nuclear structure and momentum is favored, and (2) energy must be conserved during the transition. For radiative transitions, energy is conserved during a transition by the absorption or emission of a photon ($h\nu$), which corresponds exactly to the energy difference between the initial and final states. For a radiationless transition, *the initial and final electronic states must have the same energy and the same nuclear geometry*. In other words, the initial and final states must look alike energetically and structurally.

In contrast to the situation for radiative transitions, *vertical jumps between* PE *curves separated by a large energy gap are improbable because of the need to conserve energy during a radiationless transition.* It is easiest to conserve energy for radiationless transitions *at points for which curves cross or come close together*, since at the crossing points the wave functions [e.g., ψ_1(R) and ψ_2(*R)] have exactly the same energy. Now, we can connect the quantum mechanical interpretation of radiationless transitions in terms of the FC factor ($< \chi_1|\chi_2 >$) to the motion of the representative point on a PE surface.

Suppose a molecule starts off on an excited PE curve corresponding to the electronically excited state whose electronic wave function is ψ_2(*R) and undergoes a LU → HO electronic transition to ψ_1(R). Fig. 3.4 depicts just such a situation. On the left, the molecule begins in the ψ_2(*R) state, and on the right, the molecule has just been converted to the ψ_1(R) state. The representative point of ψ_2(*R), during its zero-point motion, makes a relatively small-amplitude oscillating trajectory between points A and B on the excited surface (Fig. 3.4a). But after the transition to ψ_1(R)

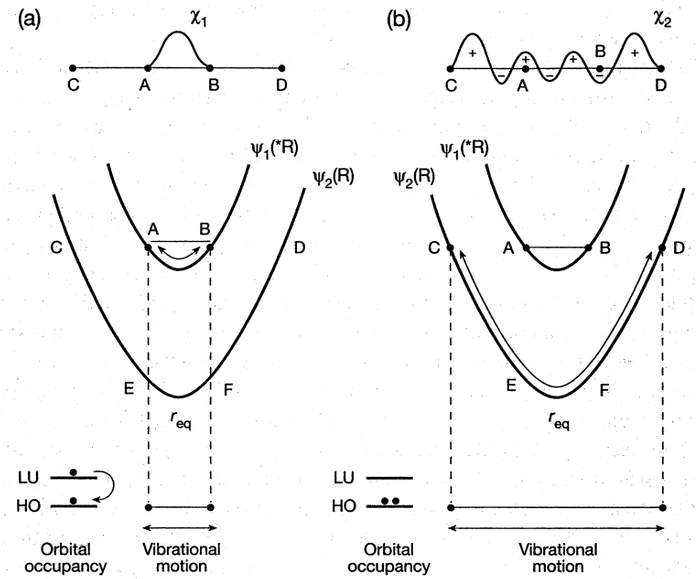

Figure 3.4 Visualization of the quantum mechanical basis for a slow rate of radiationless transitions due to low positive overlap of the vibrational wave functions.

the representative point makes a relatively large-amplitude oscillating trajectory between points C and D (Fig. 3.4b) because the electronic energy of ψ_2(*R) has been converted into the vibrational energy of ψ_1(R). For a radiationless transition from the ψ_2(*R) curve to the ground-state ψ_1(R) curve to be *possible*, energy and momentum must be conserved.

What happens when, in the limiting classical cases, a *horizontal* jump with conservation of PE occurs (Fig. 3.4a, A → C or B → D), or a *vertical* jump with conservation of geometry (Fig. 3.4b A → E or B → F) occurs? A classical horizontal "jump" from ψ_2(*R) to ψ_1(R) that conserves energy requires an unlikely abrupt change in nuclear geometry. The representative point, initially in $v = 0$ of ψ_2(*R), will be undergoing a vibration of small amplitude between A and B before and after the horizontal transition to C or D [at points C and D, the atoms on ψ_1(R) are momentarily moving slowly since they are at turning points of a vibration]. However, because the initial and final states have very different geometries, they do not "look alike" and therefore the horizontal jump is improbable. A classical *vertical* jump that conserves the initial geometry from ψ_2(*R) to ψ_1(R) will start an abrupt transformation of the representative point from a very small, mild-amplitude vibration with little KE and momentum between A and B to a very large-amplitude, high kinetic-energy oscillation between C and D. The motions of the representative points in ψ_2(*R) to ψ_1(R) do not look alike, and therefore the transition is improbable. The vertical jumps A → E or B → F

are unlikely because, in order to conserve energy, some external energy sink must be available to suddenly absorb a great deal of energy.

The net result of either a horizontal or vertical jump from $\psi_2(^*R)$ to $\psi_1(R)$ is that the vibration of the molecule will cause either an abrupt change in geometry (Fig. 3.4a) or an abrupt change in momentum (Fig. 3.4b). Thus, we can conclude that radiationless transitions between two PE curves that do not come close in energy are implausible. An abrupt change in the positional or momentum characteristics of a vibration corresponds to a large change in the organizational energy of the vibrating system. Classically, transitions requiring such large structural or dynamic reorganizations are resisted, and therefore implausible. Put in simpler terms, the initial and final state do not look very much alike in terms of their initial and final kinetic energies or of their initial and final structures, so a transition between them is slow.

Let us see how the quantum mechanical wave functions for the vibrations deal with the two transitions shown in Fig. 3.4 for the transition $\psi_1(^*R) \rightarrow \psi_2(R)$. Suppose the wave functions χ_1 and χ_2 correspond to the $v = 0$ and $v = 6$ vibrations of $\psi_1(^*R)$ and $\psi_2(R)$, respectively. The vibrational wave functions for the initial (i.e., χ_1, $v = 0$) and the final state (i.e., χ_2, $v = 6$), which are shown at the top of Fig. 3.4, do not look at all alike. That is, χ_1 is always positive (no nodes), whereas χ_2 oscillates a number of times ($v = 6$, so there are six nodes). The dissimilarities of the two wave functions immediately lead to the conclusion that the overlap integral ($< \chi_1|\chi_2 >$) will have a value close to zero because of mathematical cancellation of the two functions. The poor net overlap is shown schematically in Fig. 3.5 (left).

Now, we consider the situation for which two PE curves come very close in energy (i.e., they actually intersect). Consider the mathematical form of the vibrational wave functions χ_1 and χ_2 for the initial and final vibrations shown in Fig. 3.5 for a radiationless transition, similar to that of Fig. 3.4, in which the two surfaces are far apart for all values of r (Fig. 3.5 (left), and a radiationless transition in which the two surfaces come close together and intersect or cross at a specific value of r (Fig. 3.5, right). Recall that for a radiative or radiationless transition to be probable according to the FC principle, there must be net positive overlap between these wave functions.

By inspection of the curves in Fig. 3.5 (left), namely, the case for which the two surfaces involved in the radiationless transition are far apart for all values of r, the vibrational wave function χ_1 (positive everywhere, no node) associated with $\psi_1(^*R)$, plotted above the classical curve representing the excited state, is drastically different in form from the vibrational wave function χ_2 (highly oscillating between positive and negative values) associated with $\psi_2(R)$ at the energy where the transition occurs. Therefore, the mathematical overlap integral of χ_2 and χ_1 (i.e., $< \chi_1|\chi_2 >$), the net overlap, will be zero or close to zero, because the initial function (χ_1) is positive everywhere about the point r_{eq} (the equilibrium separation) but the final function (χ_2) oscillates between positive and negative values about r_{eq}. The result is an effective cancellation of the mathematical overlap integral (Fig. 3.5, bottom left). Quantum intuition tells us, as does the FC principle, that if the overlap integral $< \chi_1|\chi_2 >$ is very small, the probability of the radiationless transition from $\psi_1(^*R)$ to $\psi_2(R)$ will also be very small. More simply stated, the wave functions χ_1 and χ_2 do not look very much alike and will be difficult to make look alike through electronic couplings. In

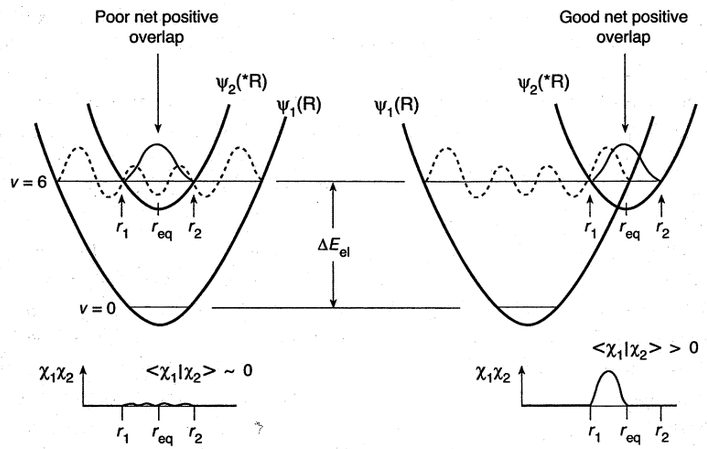

Figure 3.5 Schematic representation of situations for poor (left) and good (right) net positive overlap of vibrational wave functions. The value of the integral $< \chi_1|\chi_2 >$ as a function of r is shown at the bottom of the figure.

terms of a selection rule, the transition as shown in Fig. 3.4 is implausible and will occur at a slow rate.

In Fig. 3.5 (right), there is a specific value of r where PE *curve-crossing* occurs between the wave functions $^*\psi_1$ and ψ_2. How can visualization of the overlap of vibrational wave functions provide some quantum insight into the operation of the FC principle when two PE curves intersect one another? The poor overlap of the vibrational wave functions χ_1 and χ_2 for a molecule in the lowest vibrational level of $^*\psi_1$ for the noncrossing situation (Fig. 3.5, left) contrasts with the significant overlap for the curve-crossing situation (Fig. 3.5, right). In both cases, χ_1 corresponds to the $v = 0$ level of $^*\psi_1$ and χ_2 corresponds to the $v = 6$ level (six nodes in the wave function) of ψ_2.

The amount of electronic energy (ΔE_{12}) that must be converted into vibrational energy and the vibrational quantum number (v) of the state produced by the transition are the same for both transitions shown in Fig. 3.5. The vibrational overlap integrals $< \chi_1|\chi_2 >$ for the crossing and noncrossing situations are shown at the bottom of Fig. 3.5. The net overlap for the situation on the left is much less than that for the situation on the right. The wave function $\chi_2(v = 6)$ undergoes oscillations from mathematical plus to minus in the regions of space where the wave function $\chi_1(v = 0)$ is positive, thus causing a poor vibrational overlap integral. Consistent with the classical FC principle, therefore, quantum intuition states that radiationless transition for the surface-crossing situation (Fig. 3.5, right) will occur much faster than the nonsurface crossing, radiationless transition (Fig. 3.5, left) because the vibrational overlap integral ($< \chi_1|\chi_2 >$) is larger for the situation on the right. In terms of a selection rule, a radiationless transition when there is no surface is *Franck–Condon*

forbidden (i.e., the FC factor $< \chi_i|\chi_j >^2 \sim 0$), whereas a radiationless transition at the surface-crossing (Fig. 3.5, right) is *Franck–Condon allowed* (i.e., the FC factor $< \chi_i|\chi_j >^2 \neq 0$).

For some vibrations that distort the energy surface of *R, there are those vibrations that may be better represented by Fig. 3.5 (left) and other vibrations that may be better represented by Fig. 3.5 (right). In other words, certain vibronic interactions, Fig. 3.5 (right), can lead to radiationless transitions between states by causing energy surfaces to intersect, and thereby enhance the FC factors for transition.

In summary, *radiationless transitions are most probable when two* PE *curves for vibration cross (or come very close to one another), because when this happens, it is easiest to conserve the energy, motion, and phase of the nuclei during the transition in the region of the crossing.* In other words, in the regions of curve crossings, the wave functions of *R and R look alike structurally, energetically, and dynamically. It has been assumed that the vibrational transition, rather than the electronic transition, is rate determining. This means that the curve crossing shown in Fig. 3.5 actually would not occur because the electronic states are mixed by the vibration in the region where the crossing occurs. This case is usually for radiationless electronic transitions involving no change in spin. Such crossings are more complicated in polyatomic molecules and are discussed in Chapter 6.

3.12 Radiationless and Radiative Transitions between Spin States of Different Multiplicity[8]

The spirit of the paradigm for the selection rules for spin transitions is similar to that for electronic and vibronic transitions. As before, we postulate that for all radiative or radiationless transitions, energy and momentum must be conserved and that transitions between states of different spin are allowed or plausible only when the initial and final states look alike in terms of structure and motion.

Some of the most important examples of spin transitions in organic photochemical reactions are listed in Scheme 3.2. These transitions are analogous to the general transitions of Scheme 3.1, except they are for transitions that involve a change of spin, specifically for the conversion of a singlet state to a triplet state or vice versa.

In Scheme 3.2, we will develop a model that will make it possible to understand and visualize the mechanisms for all of the spin transitions. The pictorial model uses the vector model of spin developed in Chapter 2. A precessing vector representing the spin wave function ($\mathbf{S}$), analogous to the spirit of the pictorial model developed for vibrating nuclei or orbiting electrons, is employed. Consider the spin wave function of an initial spin state ($\mathbf{S}_1$) and a final spin state ($\mathbf{S}_2$). Analogous to the electronic overlap integral ($< \psi_1|\psi_2 >$) and the vibrational overlap integral ($< \chi_1|\chi_2 >$), there is a spin overlap integral $< \mathbf{S}_1|\mathbf{S}_2 >$. When there is no spin change during the transition, then $< \mathbf{S}_1|\mathbf{S}_2 > = 1$ (e.g., singlet–singlet, triplet–triplet, or doublet–doublet transitions). In this case, the initial and final spin states look alike in all respects and there is no spin prohibition on the electronic transition. However, when there is a spin change during the transition, $< \mathbf{S}_1|\mathbf{S}_2 > \neq 0$ (e.g., singlet–triplet transitions) and in the zero-order approximation, the transition is strictly forbidden.

(a) $R(S_0) + h\nu \rightarrow {}^*R(T_1)$
(b) ${}^*R(T_1) \rightarrow R(S_0) + h\nu$
(c) ${}^*R(T_1) \rightarrow R(S_0) + \text{heat}$
(d) ${}^*R(S_1) \rightarrow R(T_1) + \text{heat}$
(e) ${}^3I(D) \rightarrow {}^1I(D)$ and ${}^1I(D) \rightarrow {}^3I(D)$

Scheme 3.2 Some important transitions involving intersystem crossing.

In first order, transition between singlets and triplets becomes allowed only if an interaction for mixing spin states is available. In contrast to the mixing of electronic states, the mixing of spin states requires *magnetic interactions, not electrostatic interactions.* At a fundamental level, an electronic transition that involves a change of spin angular momentum requires some interaction (coupling) with another source of angular momentum that can both trigger the transition and allow conservation of the total angular momentum of the two interacting systems during the transition and provide for the conservation of *magnetic* energy. For organic molecules, the most important interaction that couples two spin states and that provides a means of conserving the total angular momentum of the system is the coupling of the electron spin with the orbital angular momentum (i.e., spin–orbit coupling).

From Scheme 3.2, the most important radiative transitions involving a spin change are the spin-forbidden absorption, $R(S_0) + h\nu \rightarrow {}^*R(T_1)$, and the spin-forbidden emission (phosphorescence), ${}^*R(T_1) \rightarrow R(S_0) + h\nu$. The most important radiationless transitions for *R involving a spin change are ${}^*R(T_1) \rightarrow R(S_0) + \text{heat}$ and ${}^*R(S_1) \rightarrow {}^*R(T_1) + \text{heat}$. Both are intersystem crossings (ISC). Primary photochemical processes, such as $^*R \rightarrow I(D)$, may be considered as elementary chemical steps for which a change of spin is forbidden by the spin selection rules. Thus, when the primary photochemical process is an ${}^*R(T_1) \rightarrow {}^3I(D)$ transition, the ISC process ${}^3I(D) \rightarrow {}^1I(D)$ shown in Scheme 3.2e must occur before products (P) can be formed from ${}^1I(D)$. This important ${}^3I(D) \rightarrow {}^1I(D)$ ISC step is discussed in Section 3.24 and in Chapter 6.

3.13 Spin Dynamics: Classical Precession of the Angular Momentum Vector[9]

In Section 2.24, we developed a model representing the electron spin angular momentum ($\mathbf{S}$) as a vector. The spin vector $\mathbf{S}$ possesses an associated magnetic moment, $\boldsymbol{\mu}_S$ (Eq. 2.32). In the absence of any other magnetic fields (i.e., other magnetic moments), both the $\mathbf{S}$ and $\boldsymbol{\mu}_S$ vectors lie motionless in space and possess a magnetic energy (E). The situation is quite different when there are magnetic fields (i.e., magnetic moments), $\mathbf{H}_z$, that couple with the magnetic moment of the electron spin, $\boldsymbol{\mu}_S$. The result of such a coupling is that the electron spin (and its associated magnetic moment, $\boldsymbol{\mu}_S$) orients itself either in a direction aligned with the coupling field ($\mathbf{H}_z$) or in a direction